Structure of C3b-factor H and implications for host protection by complement regulators

Jin Wu[1], You-Qiang Wu[2], Daniel Ricklin[2], Bert J.C. Janssen[1], John D. Lambris[2,3] & Piet Gros[1,3]

[1]Crystal and Structural Chemistry, Bijvoet Center for Biomolecular Research, Department of Chemistry, Faculty of Science, Utrecht University, Padualaan 8, 3584 CH Utrecht, The Netherlands,

[2]Department of Pathology & Laboratory Medicine, University of Pennsylvania, 401 Stellar Chance, Philadelphia, PA 19104, USA

[3]Shared senior authorship

SUPPLEMENTARY MATERIAL

Supplementary Table 1. Structural comparison of FH(1-4) with NMR structures of FH(1-2) and FH(2-3).

Supplementary Table 2. Analysis of the interfaces between C3b and FH(1-4).

Supplementary Figure 1. Structural comparison of C3b structures.

Supplementary Figure 2. Thioester containing domain of C3b and comparison with C3d.

Supplementary Figure 3. Effect of anti-C3b mAbs on FH(1-4) binding.

Supplementary Figure 4. CONSURF analysis of FH(1-4) from different species.

Supplementary Figure 5. Structural-based sequence alignment of FH, DAF and VCP.

Supplementary Figure 6. Steric hindrance between FH and the glycan attached to Asn-260 of Bb.

Supplementary Figure 7. Stereo representation of the C3b-FH(1-4) complex coloured by electrostatic potential.

Supplementary Figure 8. Detailed views of disease-linked mutations.

Supplementary Figure 9. Decay of the C3 convertase by FH(1-4).

Supplementary methods

Supplementary references

Structure of C3b-factor H(1-4)
Supplementary Figure 1

	C3b (pdb code: 2I07)		C3b (pdb code: 2ICF)	
	Translation (Å)	Rotation (°)	Translation (Å)	Rotation (°)
MG1	2.2	5.5	0.7	2.3
MG4	2.1	5.5	1.1	1.5
MG5	2.9	4.8	1.0	2.8
TED	6.9	11.8	3.7	7.5
CUB	5.2	12.9	1.4	6.0
C345C	19.2	25.8	--*	--*

	Rmsd (Cα) (Å)	
C3b core (41% of total model)	0.97	0.88

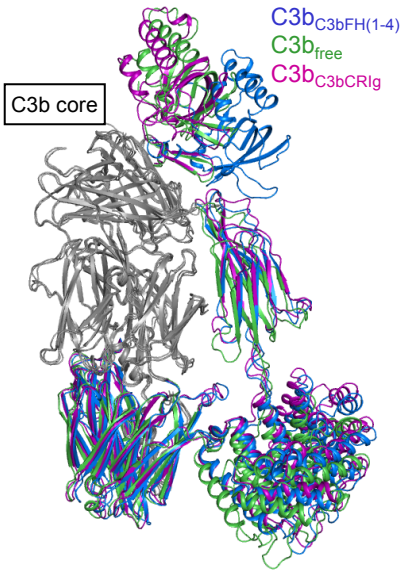

Supplementary Figure 1. Structural comparison of C3b structures.
C3b in C3b-FH(1-4) complex (blue) was superposed on the crystal structures of free C3b (pdb code: 2I07)[14] (green) and C3b in complex of CRIg (pdb code: 2ICF)[15] (magenta) based on the C3b core consisting of MG2, MG3, MG6, LNK, α'NT, MG7 and MG8 (654 residues) (grey). The values of domain translation and rotation are calculated using SUPERPOSE in the CCP4 package[51].
*) The C345C domain in C3b-CRIg structure had weak density and was not refined in the structure[15].

Structure of C3b-factor H(1-4)
Supplementary Figure 2

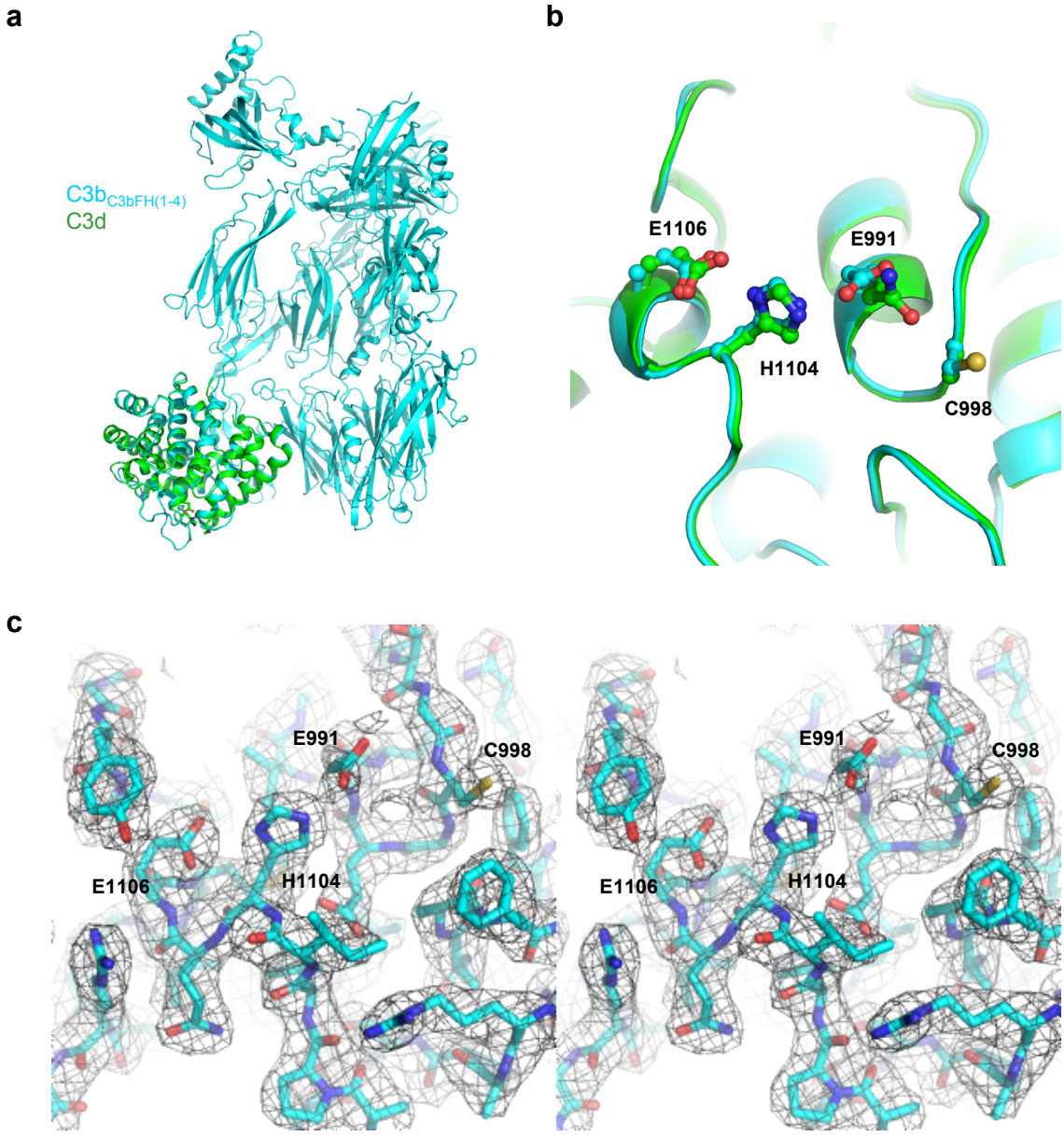

Supplementary Figure 2. Thioester containing domain of C3b and comparison with C3d. (**a**) Superposition of C3d (pdb code: 1C3D)[52] (green) with C3b in C3b-FH(1-4) complex (cyan). (**b**) Detail of thioester region. Glu-991, Cys-998, His-1104 and Glu-1106 are shown in ball-and-sticks. Cys-998 was mutated to Ala in C3d[52]. The two structures show similar conformations. C3b was treated with iodoacetamide after generation by limited trypsinization (see **Methods**). However, Cys-998 was exposed and no extra density was visible around it. (**c**) Stereo views of the electron density for the thioester region.

Structure of C3b-factor H(1-4)
Supplementary Figure 3

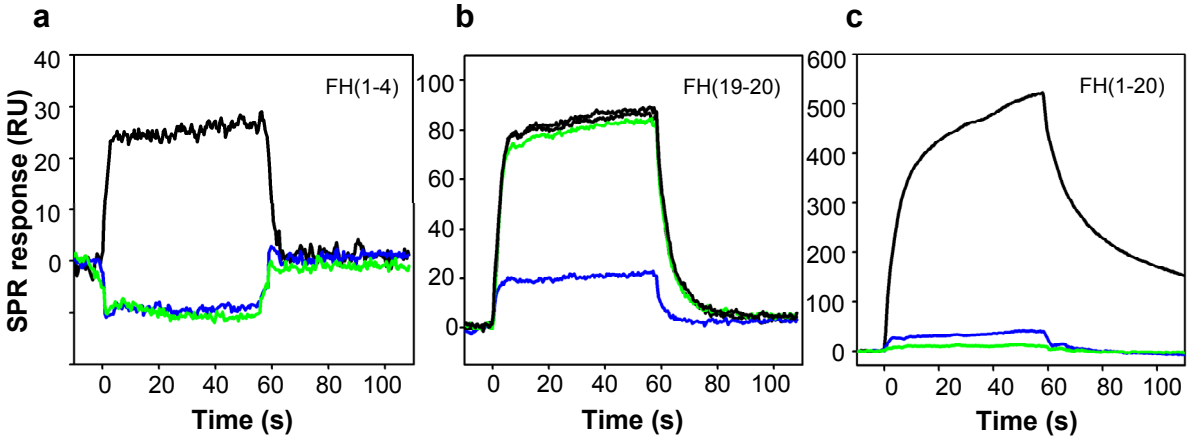

Supplementary Figure 3. Effect of anti-C3b mAbs on FH(1-4) binding.
Antibodies against specific domains of C3b were used to investigate the contribution of these domains to the binding of FH(1-4). Using SPR, the binding signals of FH(1-4)(**a**), FH(19-20)(**b**), and FH(1-20)(**c**) were assessed before (black) and after injection of the antibodies onto immobilized C3b. In case of antibody C3-9, which is directed against the MG7/8 domains of C3b[53], only the binding of FH(1-4) and FH(1-20) but not FH(19-20) was impaired (green). In contrast, the TED-specific mAb311 also affected binding of FH(19-20), which is known to interact with the TED domain (blue). This confirms that both the TED and MG7 domain are involved in the binding of C3b to FH(1-4). Data are representative of two to three experiments.

Structure of C3b-factor H(1-4)
Supplementary Figure 4

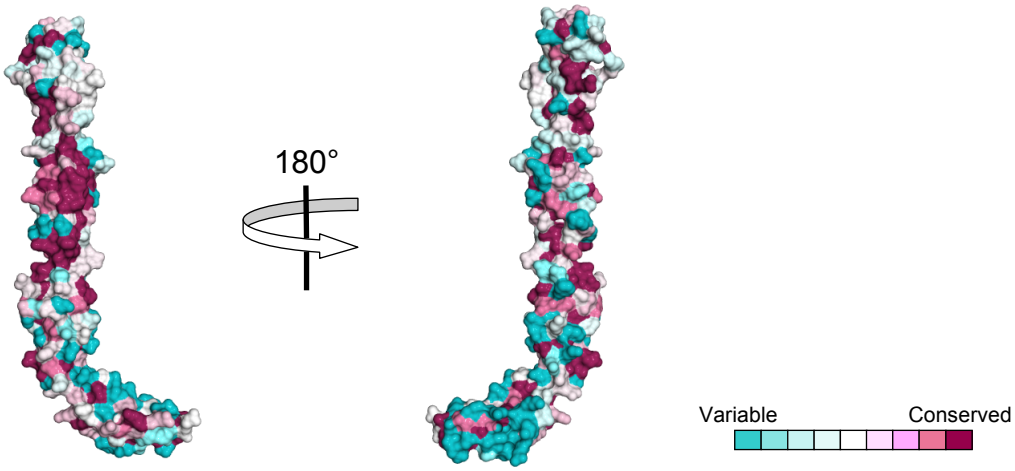

Organism	GenInfo Identifier	Similarity
Homo sapiens (human)	77744385	--
Pan troglodytes (chimpanzee)	114568537	98%
Macaca mulatta (rhesus monkey)	109018998	90%
Rattus norvegicus (Norway rat)	77861917	72%
Equus caballus (horse)	194227377	69%
Sus scrofa (pig)	47523636	67%
Canis familiaris (dog)	74005966	67%
Mus musculus (house mouse)	109627652	67%
Bos Taurus (cattle)	76677897	65%
Monodelphis domestica (opossum)	126306560	55%
Gallus gallus (red jungle fowl)	118094043	50%

Supplementary Figure 4. CONSURF analysis of FH(1-4) from different species.
FH(1-4) is presented in the similar orientation as **Fig. 2b** (top), while the right-hand side is rotated by 180°. FH(1-4) is colored according to their conservation scores (1-9 from variable to conserved) based on CONSURF analysis[54]. The color scale is indicated above. The species chosen for the sequence alignment are listed in the Table.

Structure of C3b-factor H(1-4)
Supplementary Figure 5

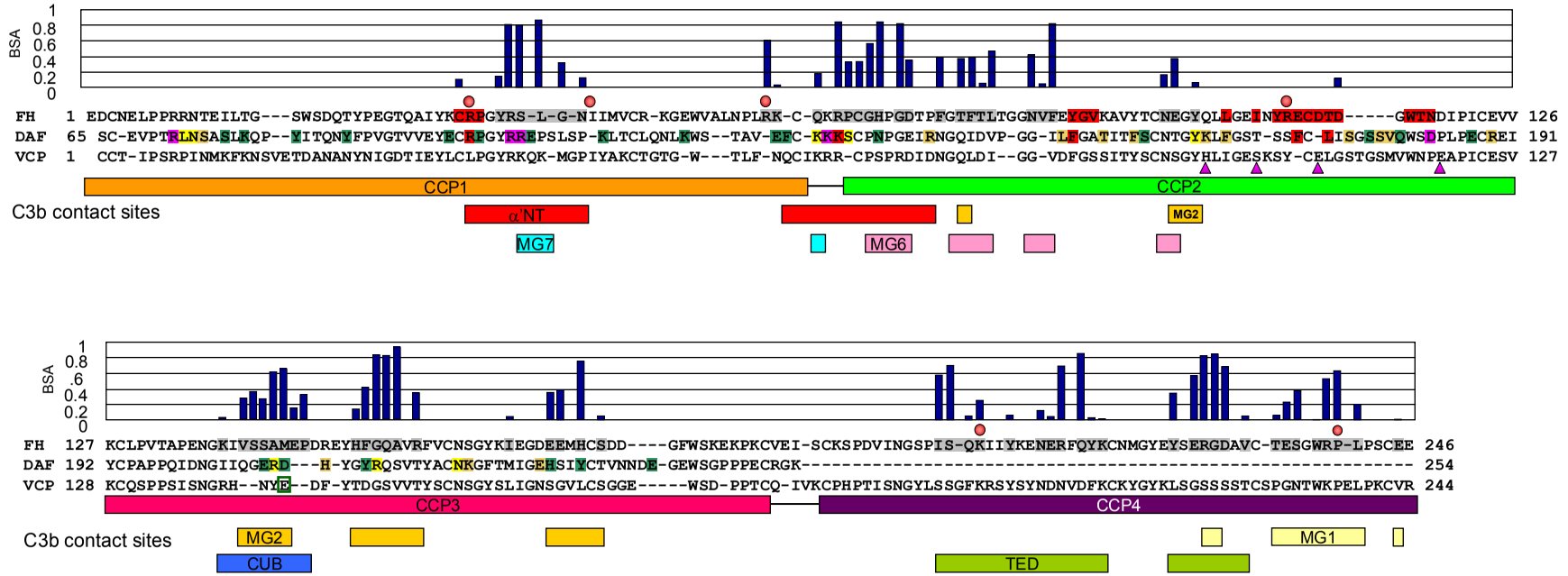

Supplementary Figure 5. Structural-based sequence alignment of FH, DAF and VCP.
FH and DAF were aligned based on crystal structures, and VCP was aligned based on sequence using ClustalW2 (www.ebi.ac.uk/Tools/clustalw2/). The residues in FH making contact to C3b are shaded in grey; vertical bars indicate the fraction of the buried solvent-accessible surface area per residue (calculated by the protein interface analysis program PISA, www.ebi.ac.uk/msd-srv/prot_int/pistart.html). The corresponding C3b contact sites are indicated by blocks at the bottom of the alignment with the same color as indicated in **Fig. 2a**. The disease-related mutants are labeled by the red dot on top of the residues, and the triangles are used to mark the important residues in VCP in cofactor activity assay based on ref. 30. Glu-144 of VCP located in the hyper-variant loop of CCP3 shows a significant effect on C3b binding (ref. 30) and is indicated by a green box. The region in FH overlapping with Bb (atomic distances shorter than 2Å) is highlighted in red. Mutations in DAF are highlighted according to the functional data in ref. 24 (red: critical for decay accelerating activity; magenta: severe effects on activity; yellow: medium effects, beige: minor effects; green: subtle or no effects).

Nature Immunology: doi:10.1038/ni.1755

Structure of C3b-factor H(1-4)
Supplementary Figure 6

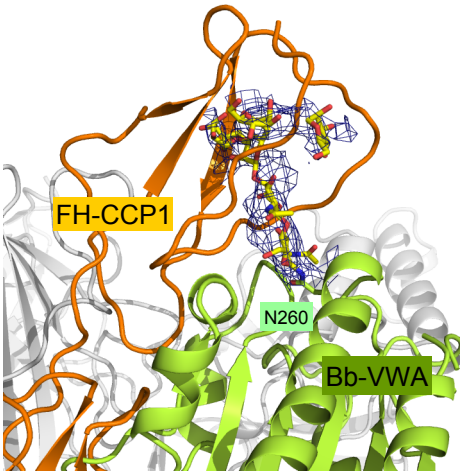

Supplementary Figure 6. Steric hindrance between FH and the glycan attached to Asn-260 of Bb. C3b-FH(1-4) was superposed on the C3 convertase model[21] as shown in **Fig. 4a**. FH CCP1 clashes with the glycan attached to Asn-260 in the VWA domain of Bb. Electron density (*2Fo-Fc* map contoured at 1σ) of this glycan is shown.

Structure of C3b-factor H(1-4)
Supplementary Figure 7

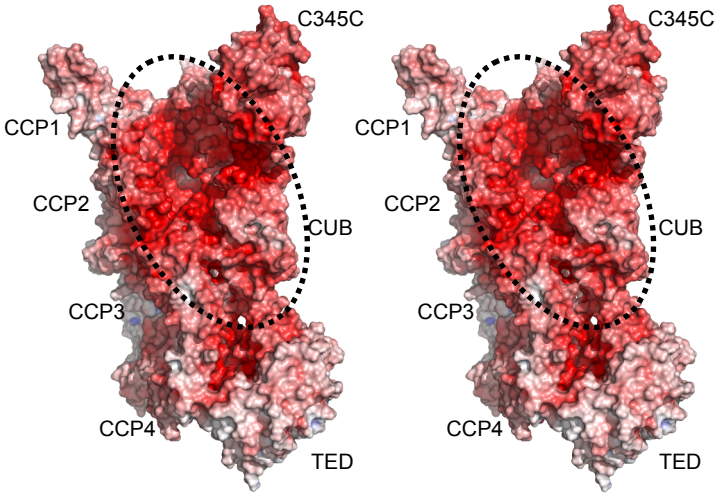

Supplementary Figure 7. Stereo representation of the C3b-FH(1-4) complex coloured by electrostatic potential.
The potential contours are shown on a scale from -15 (red) to + 15 $k_bTe_c^{-1}$ (blue). The dotted oval indicates the proposed FI binding region formed by FH domains CCP1-3 and C3b domains CUB and C345C.

Structure of C3b-factor H(1-4)
Supplementary Figure 8

a

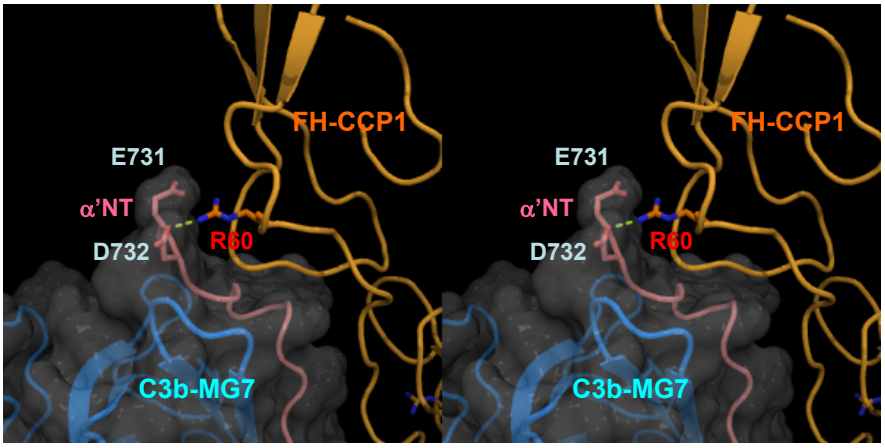

b

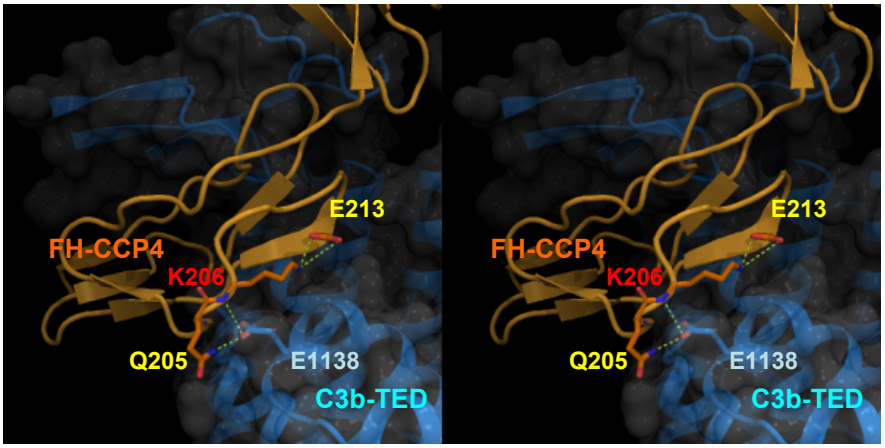

c

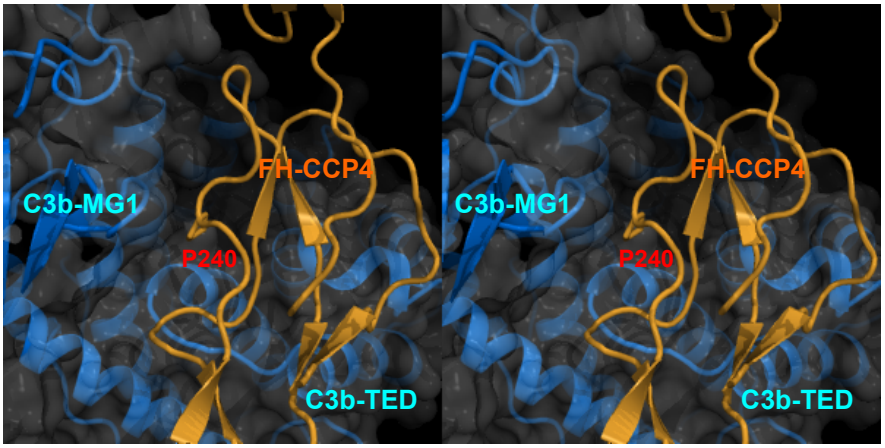

Structure of C3b-factor H(1-4)
Supplementary Figure 8

d

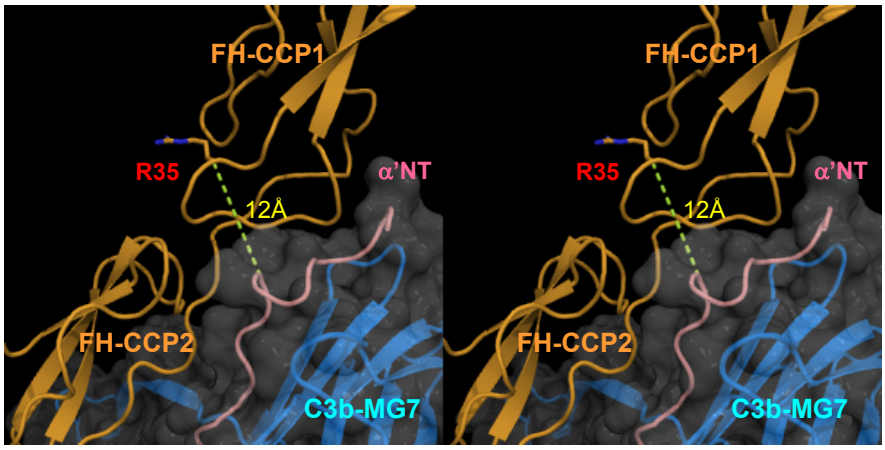

e

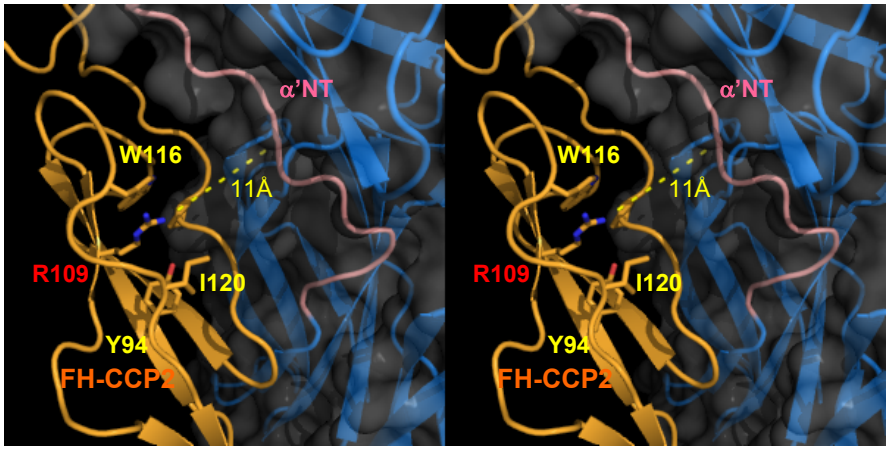

f

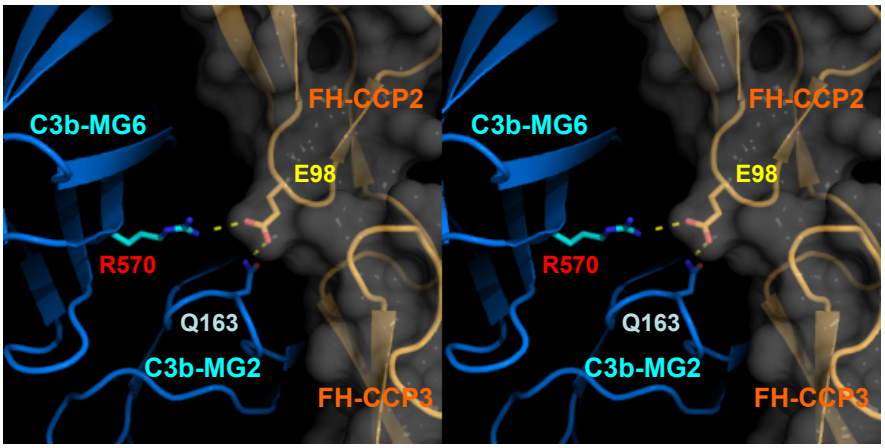

Structure of C3b-factor H(1-4)
Supplementary Figure 8

g

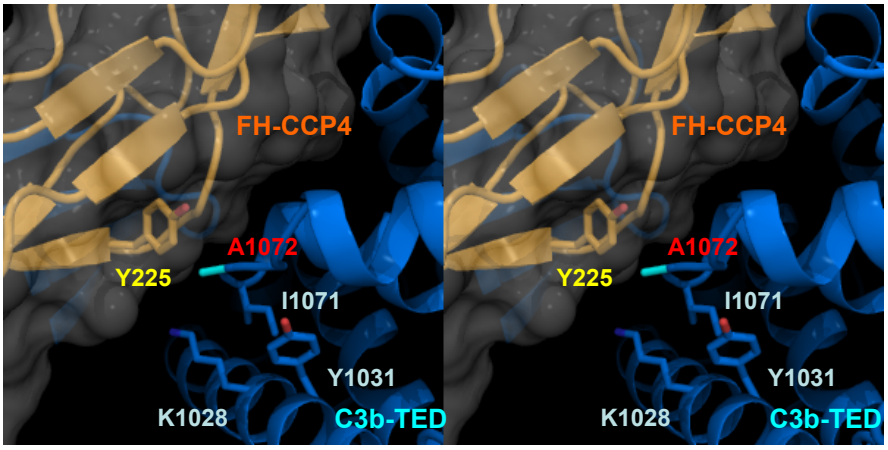

h

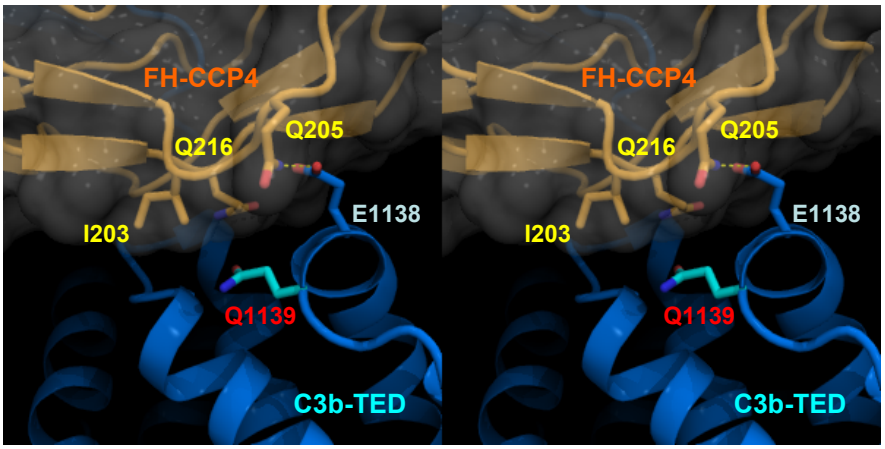

Supplementary Figure 8. Detailed views of disease-linked mutations.
Stereo views of FH residues Arg-60[35] (**a**), Lys-206[32] (**b**), Pro-240[33] (**c**), Arg-35[33] (**d**) and Arg-109[39] (**e**). Arg-60, Lys-206 and Pro-240 are at the C3b interface, while Arg-35 and Arg-109 are more than 10 Å away from the complex interface. (**f**), (**g**) and (**h**) are the stereo views of residues Arg-570, Ala-1072 and Gln-1139 in C3b[34].

Structure of C3b-factor H(1-4)
Supplementary Figure 9

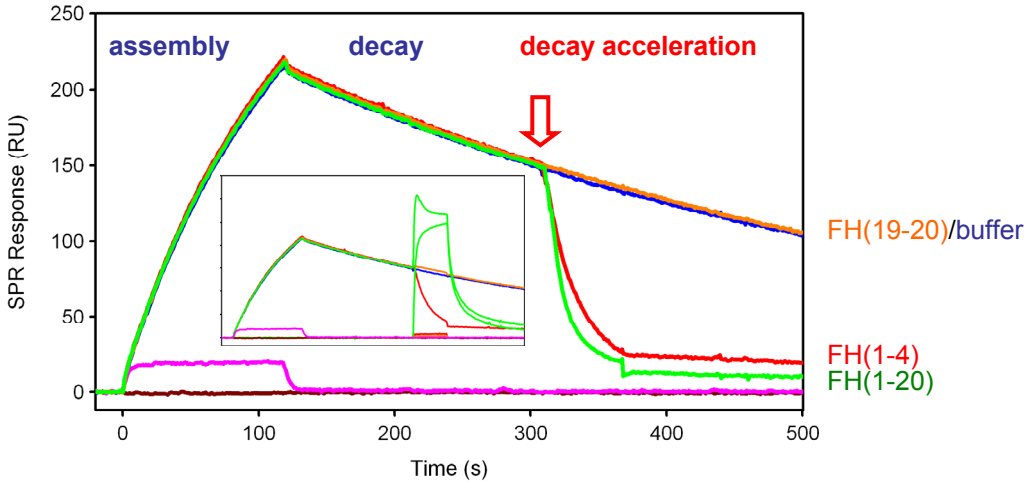

Supplementary Figure 9. Decay of the C3 convertase by FH(1-4).
Formation, decay, and decay acceleration of the alternative pathway C3 convertase was monitored by SPR. The C3 convertase complex (C3bBb) was formed by injecting a mixture of FB and factor D (FD) on immobilized C3b. Only the combined factors but not FB (magenta) or FD (brown) alone led to the assembly of a stable complex. After observing regular convertase decay for 3 min, either FH(1-20) (green), FH(1-4) (red), FH(19-20) (orange), or buffer (blue) was injected for 1 min and the drop in post-injection signal was evaluated for decay acceleration. While FH(19-20) did not affect convertase decay, FH(1-4) accelerated the decay to a similar extent as FH(1-20). Extended analysis from **Fig. 1d**. Binding data for convertase assay are representative of three individual experiments (controls with pure FB or FD were injected twice).

Structure of C3b-factor H(1-4)
Supplementary Table 1

	FH(1-2) (pdb code: 2RLP)		FH(2-3) (pdb code: 2RLQ)	
	Translation (Å)	Rotation (°)	Translation (Å)	Rotation (°)
CCP1	3.5	9.3	--	--
CCP3	--	--	3.2	9.5
	Rmsd (Cα) (Å)			
CCP2	1.3		1.1	

Supplementary Table 1. Structural comparison of FH(1-4) with NMR structures of FH(1-2) and FH(2-3).
Superposition of FH(1-4) from the C3b-FH(1-4) complex and NMR structures of FH (1-2) and FH (2-3)[12] based on the CCP2 domains (see **Fig. 2b**, top). The values of domain translation and rotation were calculated using SUPERPOSE in the CCP4 package[51].

Structure of C3b-factor H(1-4)
Supplementary Table 2

Interface		Buried area (Å)	$^{i}N_{res}$		N_{HB}	N_{SB}	$\Delta^{i}G$ Kcal/mol	$\Delta^{i}G$ P-value
			C3b	FH				
C3b	FH(1-4)	4485	79	68	21	8	-4.1	0.609
C3b	CCP1	838	15	9	6	1	-0.4	0.539
C3b	CCP2	1009	22	18	1	1	-2.6	0.575
C3b	CCP3	1239	24	20	7	4	-2.8	0.440
C3b	CCP4	1472	24	21	7	2	-1.0	0.635

Supplementary Table 2. Analysis of the interfaces between C3b and FH(1-4).
All values are calculated by PISA (www.ebi.ac.uk/msd-srv/prot_int). The buried area is calculated as difference in total accessible surface areas of isolated and interfacing structures. $^{i}N_{res}$ indicates the number of residues at the interface. The N_{HB} and N_{SB} indicates the number of potential hydrogen bonds and salt bridges across the interface, respectively. $\Delta^{i}G$ indicates the solvation free energy gain upon formation of the interface. $\Delta^{i}G$ P-value indicates the P-value of the observed solvation free energy gain.

Supplementary Methods

Generation and purification of the C3b fragment

1 mg/ml purified C3 was treated with 1% (w/w enzyme/substrate) trypsin for 2 min at 37 °C in phosphate buffered saline (PBS). 5% (w/w inhibitor/substrate) soybean trypsin inhibitor was added to stop the reaction and the protein sample was transferred on ice immediately, followed by treatment with 20 mM iodoacetamide for 30 min. The C3b sample was diluted 1:1 with 25 mM Tris, 50 mM NaCl, pH 8.0 and loaded on a Mono-Q HR 5/5 (1 ml) column, equilibrated in 25 mM Tris, 100 mM NaCl, pH 8.0, and eluted with a linear gradient of 100-300 mM NaCl over 30 column volumes. The fractions containing C3b were pooled, concentrated and further purified by a Superdex 200 HR 10/30 column. The purified C3b sample was dialyzed against 10 mM Tris, 50 mM NaCl, pH 7.4, concentrated to 30 mg/ml, and stored at -80 ºC. The purity of C3b was verified using SDS-PAGE.

Binding affinity assay

All surface plasmon resonance (SPR) studies were performed on a Biacore 2000 instrument (GE Healthcare Corp., Piscataway, NJ) at 25 °C. Binding signals were processed and evaluated using Scrubber (version 2; BioLogic Software Pty. Ltd., Campbell, Australia). The direct binding of FH(1-4) to C3b was assessed by capturing thioester-specifically biotinylated C3b (30 μg ml^{-1}) to a streptavidin-coated sensor chip (SA chip; GE Healthcare) at various surface densities (3,000-7,000 resonance units; RU) and injecting a twofold dilution series of recombinant FH(1-4) (20-0.02 μM) for 1 min. at a flow rate of 20 μl min^{-1} in 10 mM PBS-T pH 7.4 (10 mM sodium phosphate, 150 mM NaCl, 0.005% Tween-20). Owing to the rapid dissociation rate, no regeneration was required between injections. A blank streptavidin surface was used as a reference and an ensemble of buffer blank injections was subtracted from the data sets to eliminate injection artifacts[49]. The apparent equilibrium dissociation constant (K_D) was calculated

Nature Immunology: doi:10.1038/ni.1755

as an average of six data sets by plotting the steady state signals of FH(1-4) injections against the concentration and fitting individual data sets to a single-binding-site model.

Antibody competition assay

The ability of anti-C3c or anti-C3d mAbs to block the binding of FH fragments to C3b was investigated by SPR using a Biotin CAPture sensor chip (prototype kit; GE Healthcare Corp.) and PBS-T as running buffer. Streptavidin was loaded on the chip surface by injecting a conjugate solution (50 μg/ml) for 5 min at 2 μl/min on all four flow cells. Biotinylated C3b (30 μg/ml; 5 min) was then injected on two of the streptavidin-coated flow cells, resulting in surface densities of 2,500-3,000 RU. All surfaces were stabilized by three consecutive 30 s injections of 1 M NaCl and equilibrated for 10 min. A buffer blank (control) or 10 μg/ml of mAb 311 (anti-C3d)[16] or mAb C3-9 (anti-C3c)[16] were injected on a single C3b surface for 5 min to form the corresponding mAb-C3b complex. 1 μM recombinant FH(1-4) and FH(19-20) were each injected for 1 min at 20 μl/min, and their differential signal intensities were compared between the mAb-C3b complexes and the C3b control surface. A plain streptavidin-coated flow cell served as a reference. Buffer blank injections before and after each FH fragment sample were subtracted for compensating injection artifacts and drifting baselines on the mAb-C3b complex surfaces. At the end of each injection cycle, captured streptavidin was removed by injecting a regeneration solution (6 M guanidine-HCl in 0.25 M NaOH) for 2 min, and the chip was equilibrated in running buffer for 5 min.

mAb 311 and C3-9 were kindly provided by J. Tamerius (Cytotech) and C.E. Hack (Central Laboratory of the Netherlands Red Cross Blood Transfusion Service, The Netherlands), respectively.

Nature Immunology: doi:10.1038/ni.1755

Supplementary References

51. The CCP4 suite: programs for protein crystallography. *Acta Crystallogr D Biol Crystallogr* **50**, 760-763 (1994).

52. Nagar, B., Jones, R.G., Diefenbach, R.J., Isenman, D.E. & Rini, J.M. X-ray crystal structure of C3d: a C3 fragment and ligand for complement receptor 2. *Science* **280**, 1277-1281 (1998).

53. Nishida, N., Walz, T. & Springer, T.A. Structural transitions of complement component C3 and its activation products. *Proc Natl Acad Sci U S A* **103**, 19737-19742 (2006).

54. Landau, M. *et al.* ConSurf 2005: the projection of evolutionary conservation scores of residues on protein structures. *Nucleic Acids Res* **33**, W299-302 (2005).

Nature Immunology: doi:10.1038/ni.1755